C44

Object-related tuning of local field potentials in the premotor and primary motor cortex of an awake, behaving monkey

R.L. Spinks[1], T. Brochier[1], A. Umilta[2] and R.N. Lemon[1]

[1]*Sobell Department, Institute of Neurology, London, UK and* [2]*Dipartimento di Neuroscienze, Universita di Parma, Parma, Italy*

In the macaque monkey, both ventral premotor cortex (area F5) and primary motor cortex (M1) are part of a cortico-cortical circuit controlling grasp. F5 neurones encode the selection of various types of grasping actions, and also respond to visual presentation of graspable objects. F5 may exert its actions on the hand through cortico-cortical connections to M1, which has a major corticospinal output to hand and arm muscles. Here we compared local field potential (LFP) activity in F5 and M1 in an awake, behaving macaque performing a visuomotor task. LFPs provide a population measure of synaptic activity within an area. Surgeries to implant a head restraint device and cortical recording chambers were performed under deep anaesthesia, induced with 10 mg kg^{-1} ketamine i.m. and maintained with 2-2.5% isoflurane in 50:50 O_2:N_2O; full aseptic procedures were observed and antibiotics and analgesics given postoperatively. The task was as follows: six differently shaped objects were mounted individually on horizontal, spring-loaded shuttles, on a carousel. When two touch pads were depressed by the monkey, one object was presented visually. After a variable delay, the monkey was cued to reach for, grasp, pull and hold the object for 1s. LFPs were recorded simultaneously on multiple single microelectrodes in both F5 and M1 during 30 recording sessions; in all 144 LFPs were analysed. During both object observation and object grasp LFP power was dominated by 18-35 Hz (beta) power. LFPs were classified using post hoc analysis of the total beta power present during both object observation and steady grasp, (Student-Neumann-Keuls test, $P<0.05$) as either highly tuned (showing significantly higher power for a single object), moderately tuned (significant object tuning, but for >1 object), or untuned (no significant tuning for different objects). The total beta power in each LFP for each object was measured, and objects ranked from "best" to "worst", the best being the most preferred object.

Both areas showed distinct object-related tuning. During object presentation, a higher proportion of F5 LFPs showed tuning than did those in M1. During grasp, this was reversed. In general, M1 LFPs were more likely to be highly tuned than F5 LFPs (all comparisons, χ^2 test, $P<0.05$). The two areas had similar patterns of object preferences as a whole, but each LFP recording showed a characteristic order. The order of preference for the objects was not conserved from observation to grasp, either for individual LFPs or for whole areas.

Thus 18-35 Hz LFP power in F5 is object-tuned prior to movement onset as well as during movement execution, and this parallels single neurone data reported previously. F5 LFPs exhibit a broader range of preferred objects than M1 and more sites showed tuning during observation; although there is some premovement tuning in M1, the predominant effect is during grasp, when all M1 LFPs were tuned to some extent. These results are consistent with a role of F5 in selecting an appropriate action, which is executed via M1.

Supported by The Wellcome Trust

Where applicable, the experiments described here conform with Physiological Society ethical requirements.

C45

Effects of 5-hydroxytryptamine on dorsal vagal neurons via a TASK-like conductance

S. Hopwood and S. Trapp

Anaesthetics & Intensive Care, Imperial College London, London, UK

Dorsal vagal neurons (DVN) receive serotonergic inputs from higher CNS centres (e.g. medullary raphé nuclei) suggesting that 5-HT may exert fine modulation of vagal activity. Previous studies have shown that 5-HT increases DVN excitability in part by inhibition of a K^+ current via postsynaptic activation of $5\text{-}HT_{2A}$ receptors [1,2]. As mRNA for the two-pore-domain K^+ channels TASK and TREK has been found in DVN [3] we investigated a possible contribution of these channels to the 5-HT-inhibited K^+ conductance using whole-cell patch-clamp techniques.

Brainstem slices (200 μm) were obtained from 8-25 day-old Sprague-Dawley rats after anaesthesia (halothane). Following recovery at 34°C for 60 min, slices were maintained in ACSF (in mM: 3 KCl, 118 NaCl, 25 $NaHCO_3$, 1.2 NaH_2PO_4, 1 $MgCl_2$, 1.5 $CaCl_2$, 10 glucose; pH 7.4) at RT. Recordings from DVN were established using borosilicate glass electrodes (3-6 MΩ) filled with (in mM): 120 K-gluconate, 1 NaOH, 1 $MgCl_2$, 1 $CaCl_2$, 10 HEPES, 5 BAPTA, 2 K_2ATP, pH 7.3. Membrane properties were monitored with repetitive 1 s voltage ramps from a holding potential of -20 mV to -120 mV. All values are given as mean ± s.e.m.

In current clamp in ACSF, 5-HT (20 μM) elicited a depolarisation by 5.1 ± 1.5 mV (n=7) and an increase in firing rate. In voltage clamp, 5-HT (20 μM) reduced the standing outward current (I_{SO}) at -20 mV by 65 ± 12 pA (n=9), inhibiting a conductance (reversal: -95 ± 4 mV, n=8) which displayed Goldman-Hodgkin-Katz outward rectification, supportive of a TASK-like K^+ current.

Since TASK channels are modulated by extracellular pH, we investigated the pH-sensitivity of I_{SO} in DVN. Voltage clamp recordings were performed in HEPES-buffered ACSF (in mM: 3 KCl, 118 NaCl, 1 $MgCl_2$, 1.5 $CaCl_2$, 25 HEPES, 10 glucose; pH adjusted with NaOH). At pH 7.3, DVN exhibited an I_{SO} of 144 ± 22 pA (n=14) at -20 mV. Acidification of the ACSF to pH 6.3 reduced I_{SO} to 86 ± 14 pA (n=13), whereas raising extracellular pH to 8.5 increased I_{SO} to 219 ± 31 pA (n=15). At pH 8.5, $BaCl_2$ (1 mM) inhibited I_{SO} by 115 ± 37 pA (n=6). I_{SO} was unaffected by $ZnCl_2$ (100 μM) at pH 7.3 (n=4).

5-HT (10 μM) reduced I_{SO} by 122 ± 18 pA (n=5) at pH 7.3, whereas at pH 6.3 the 5-HT-induced inhibition of I_{SO} was 74 ± 7% (n=5) smaller.

The present data show that the excitatory effects of 5-HT on DVN may be mediated in part by inhibition of a TASK-like, pH-sensitive K^+ conductance. The pharmacological profile of I_{SO} suggests that TASK-1 (rather than TASK-3 or TREK) current is inhibited by 5-HT.

Albert AP et al. (1996). *Br J Pharmacol* **119,** 519-526.

Browning KN & Travagli RA (1999). *Br J Pharmacol* **128,** 1307-1315.

Talley EM et al. (2001). *J Neurosci* **21,** 7491-7505.

This work was supported by an MRC Career Development Award to ST.

Where applicable, the experiments described here conform with Physiological Society ethical requirements.

C46

Impaired hippocampal mossy fibre long-term potentiation in the R6/2 mouse model of Huntington's disease and in complexin II knockout mice

H.E. Gibson[1], A.J. Morton[1] and S. Jones[2]

[1]Department of Pharmacology, University of Cambridge, Cambridge, UK and [2]Department of Anatomy, University of Cambridge, Cambridge, UK

Huntington's disease (HD) is an inherited neurodegenerative brain disorder characterised by motor, emotional and cognitive abnormalities. The R6/2 transgenic mouse model of HD (Mangiarini et al. 1996) develops a progressive neurological phenotype with deficits in both motor and cognitive behaviours, including impairments in spatial learning. One possible cellular mechanism underlying learning is long-term potentiation (LTP), a form of synaptic plasticity. Synaptic dysfunction may be a feature of HD because in R6/2 mice neuronal levels of complexin II, a pre-synaptic SNARE (soluble N-ethylmaleimide-sensitive fusion protein attachment protein receptor)-complex-associated protein, are reduced in the hippocampus, a brain region involved in spatial learning. Since knockout mice lacking complexin II (*Cplx2* KO mice) also show deficits in spatial learning tasks, we hypothesised that a reduction in complexin II may contribute to abnormal hippocampal mossy fibre LTP, a form of synaptic plasticity dependent on presynaptic mechanisms.

Hippocampal slices were prepared from humanely killed wild-type (WT) and transgenic (R6/2, *Cplx2* WT and *Cplx2* KO) mice aged between 6 and 20 weeks of age. *Cplx2* mutant mouse lines were obtained from the Max-Planck-Institute for Experimental Medicine. All experiments were carried out in accordance with the UK Animals (Scientific Procedures) Act 1986 and conformed to local ethical guidelines. Electrically evoked field excitatory postsynaptic potentials (fEPSPs) were recorded in the CA3 subfield of hippocampal slices in the presence of 50 μM picrotoxin. High frequency stimulation (HFS, 3 x 100 Hertz, 1 second duration, 20 second interval) induced N-methyl-D-aspartate (NMDA) receptor-independent mossy fibre LTP that was measured between 30 and 50 minutes post-HFS in control mice (WT 187 ± 17.4%, n = 23; *Cplx2* WT 178 ± 8.80%, n = 9). However, mossy fibre LTP was significantly reduced in R6/2 mice (94.9 ± 5.66%, n = 19; p = <0.0001) and in *Cplx2* KO mice (93.5 ± 6.47%, n = 10; p = <0.0001). (All data represent mean values ± the standard error of the mean, where 'n' represents the number of slices used). Data were subjected to unpaired, two-tailed t-tests to determine statistical significance, with the use of Welch's correction where unequal variances existed between groups. These findings suggest that complexin II is required for the induction of mossy fibre LTP, and support the idea that loss of complexin II from the R6/2 mouse hippocampus contributes to impairments in mossy fibre glutamatergic synaptic plasticity.

Mangiarini L et al. (1996). Cell 87, 493-506.

This work was supported by the Hereditary Disease Foundation (USA) and the MRC.

Where applicable, the experiments described here conform with Physiological Society ethical requirements.

C47

Excitatory and inhibitory components of postsynaptic currents in the rat hippocampus

L. Magazanik, S. Buldakova, K. Kim and D. Tikhonov

Sechenov Inst. of Evolutionary Physiology and Biochemistry RAS, St. Petersburg, Russian Federation

Synaptic currents (PSC) evoked in hippocampal neurons by stimulation of Schaffer collateral are the sum of excitatory (EPSC) and inhibitory (IPSC) components. Inhibition of glutamate or GABA receptors is used for separation of the components (Karnup & Stelzer, 1999). However, such treatment affects the communication network in the slice. We employed an approach based on the difference in the reversal potentials of glutamate-gated and GABA-gated currents (Quardouz & Lacailee, 1997). Transverse slices were prepared from brains of rats decapitated under urethane anaesthesia (1g/kg, i.p.). The pipette solution for patch clamp recording contained (mM): K-gluconate-130, NaCl-5, MgCL2-2, CaCl2-1, HEPES-KOH-10, EGTA-10, MgATP-2, QX-314chloride-6. NMDA receptors were inhibited by APV. Under these conditions the reversal potential for the glutamate-gated current is about 0mV and for the GABA-gated current is about -40mV. The current-voltage curves are linear at negative voltages.

PSC from pyramidal cells and interneurons in the slice at -40mV, (close to IPSC equilibrium potential) represent EPSC(-40). PSC at -80mV, is the sum of the doubled EPSC(-40) and the IPSC(-80). This allows us to obtain IPSC(-80) as PSC(-80)-2*PSC(-40). Importantly, both EPSC(-40) and IPSC(-80) are 40mV away from their reversal potential. Thus, our approach allows separate analysis of EPSC and IPSC without pharmacological treatment. The approach was tested by analysis of the action of $GABA_A$ receptor antagonist bicuculline. Bicuculline (10 μM) inhibited 80-90% of calculated IPSCs without significant effect on EPSCs. In the pyramidal neurons both EPSCs and IPSCs were well pronounced (the ratio of amplitudes is 1.47, n=17). In contrast, in interneurons EPSC/IPSC was 2.3 on average. In 8 from 18 cells tested the inhibitory currents were negligibly small. This difference correlates with the ratios of glutamate- and GABA-evoked currents in isolated pyramidal neurons (1.1, n=14) and interneurons (1.8, n=31).

IEM-1460, a dicationic derivative of adamantine is known as selective channel blocker of Ca2+-permeable AMPA receptors (Magazanik et al., 1997). Using the approach for separate analysis of EPSC and IPSC we found that IEM-1460 does not affect both these components in hippocampal pyramidal neurons. It means that inhibitory interneurons, which form synapses on the pyramidal neurons, express low-sensitive GluR2-containing AMPARs. Contrary, recordings from interneurons of CA1 area revealed that IEM-1460 significantly reduces both EPSC (40 ±2%, n=7) and IPSC (49±13%, n=8). It is suggested that hippocampal interneurons expressing GluR2-lacking AMPARs inhibit other interneurons rather than pyramidal neurons.

Karnup S and Stelzer A. (1999) J. Physiol. 516: 485-504.

Magazanik LG et al. (1997) J. Physiol. 505: 655-663.

Ouardouz M and Lacailee JC. (1997) J. Neurophysiol. 77: 1939-1949.

Supported by RFBR grants 01-04-49353 and 02-04-49737, Wellcome Trust 067496/Z/02Z, Russian scientific schools (2222.2003.4), MCB RAS.

Where applicable, the experiments described here conform with Physiological Society ethical requirements.

C48

Voltage pulse potentiation of mEPSC amplitudes in rat CA1 pyramidal neurones requires postsynaptic membrane fusion events

A.W. Baxter and D.J. Wyllie

Neuroscience, University of Edinburgh, Edinburgh, UK

A relatively small proportion of synapses are potentiated in individual CA1 pyramidal neurones following conventional long-term potentiation (LTP) stimulating protocols. This makes it difficult to detect changes in the amplitudes of mEPSCs which would indicate that changes in synaptic efficacy are mediated, in part, by alterations in the numbers of AMPA receptors. Thus, to mimic the LTP-like postsynaptic calcium concentration change that occurs following NMDA receptor activation, we have used a depolarising voltage pulse (VP) stimulating protocol to increase intracellular calcium levels via L-type calcium channels. Neonatal rats (postnatal day 7-10) were killed by decapitation, with Home Office authority, and hippocampal slices were prepared for organotypic cell culture. In whole-cell patch-clamp recordings from CA1 neurones in slices cultured for 7-14 days we observed that mean mEPSC amplitudes increased from 21.2 ± 1.6 pA to 45.1 ± 2.2 pA, following VP stimulation (n = 25; mean ± SEM; P<0.01 Mann-Whitney U test)). VP potentiation was not associated with significant changes in the frequency of events (control 1.1 ± 0.3 Hz; VP 0.8 ± 0.2 Hz; P>0.05).

To assess whether the increase in amplitude of mEPSCs requires the insertion of AMPA receptors into postsynaptic sites we inhibited the actions of several proteins involved in intracellular membrane fusion events. In all experiments, inhibitors were included in the patch-pipette to restrict their actions to the postsynaptic cell. We observed that both N-ethylmaleimide (5 mM, n=6) and botulinum toxin A (10 ng/ml, n=7) blocked the induction of VP potentiation while interleaved control experiments showed typical potentiation. Pep2m (50 μM), a peptide that blocks the NSF binding site on the C-terminus of the GluR2 AMPA receptor subunit (Nishimune *et al.* 1998), similarly blocked VP potentiation, while a scrambled version of this peptide, Pep4c (50 μM), failed to block potentiation (control mEPSC amplitude 22.9 ± 1.6 pA, n=5; Pep2m 24.2 ± 1.6 pA, n=8; Pep4c 48.3 ± 4.5 pA, n=8). Next we examined the effects of Pep-AVKI (50 μM) to explore the possible involvement of PICK-1 in VP potentiation. This peptide also blocked potentiation (control 17.1 ± 1.2 pA; Pep-AVKI 19.5 ± 2.4 pA, n=8). None of the peptides examined altered mean mEPSC amplitude (or frequency) in recordings where they were included in the patch-pipette but no voltage-pulses were applied.

We conclude that VP potentiation shares common expression mechanisms with NMDA receptor-dependent LTP. The VP protocol provides a valuable method for studying biochemical changes in individual neurones following changes in synaptic strength.

Nishimune *et al.* (1998) *Neuron* **21**, 87-97

This work was supported by a BBSRC Committee Studentship to AWB

Where applicable, the experiments described here conform with Physiological Society ethical requirements.

C49

Characterization and network properties of neurogliaform neurons in the CA1 stratum lacunosum moleculare

C. Price and M. Capogna

MRC Anatomical Neuropharmacology Unit, Oxford, UK

We have used whole cell patch clamp recordings from visually identified neurogliaform (NG) neurons in the stratum lacunosum moleculare (slm) of are CA1 in rat 300 μm hippocampal slices to examine the network properties of these neurons. Slices were obtained from rats anaesthetized with 4% isoflurane and decapitated. During recordings neurons were filled with biocytin to allow anatomical identification of recorded cells. In some experiments cytoplasm was harvested and used in multiplex PCR reactions for the biochemical characterization of the recorded neurons. Data values represent means ± SEM.

NG neurons received monosynaptic, short latency (5.4 ± 0.32 ms; n=20), low SD of the mean latency i.e. jitter (268 ± 92 μs; n=9), 6,7-dinitroquinoxaline-2,3-dione (DNQX)-sensitive excitatory inputs directly from the perforant path input to CA1. Single cell RT-PCR revealed that these neurons were GABAergic and the majority expressed mRNA for neuropeptide Y (12/15) while only 2 of 11 non-NG interneurons expressed this mRNA. Immunocytochemically, NG neurons expressed the actin binding protein alpha actinin 2 (5/6).

Results from 34 paired recordings performed between adjacent NG neurons showed that 85% of pairs were electrically connected, with a coupling coefficient of 9.26 ± 1.08% (n=26). The presence of electrical coupling allowed the transmission of 7Hz sine waves between neurons, while 20 and 40 Hz waveforms were attenuated more. Spike synchronization between the most strongly coupled neurons was also apparent. In addition to electrical coupling, 70.5% of pairs were also chemically connected displaying a highly reliable bicuculline sensitive IPSC with a characteristic slow decay time constant (42 ± 4 ms, n=23).

Characteristic among chemically connected NG pairs was a strong depression of the synaptic response seen with 5Hz stimulation (second IPSC 42 ± 5% of the first IPSC, n=15). This depression was significantly inhibited by the selective GABAB antagonist CGP 55845 (5 μM; second IPSC 73 +/- 11% of the first IPSC; p<0.05 ANOVA with Bonferroni's Multiple Comparison Test). CGP 55845 also significantly increased the amplitude of the IPSC responding to the first pulse in a 5 Hz train stimulus by 30 ± 11% (p<0.01 Paired t-test; n=15), suggesting a tonic inhibition of synaptic transmission in addition to activity dependent inhibition. Ultrastructural localization for the GABABR1 subunits at NG synapses confirmed the presence of these receptors on NG neurons, with both postsynaptic and presynaptic extrasynaptic labelling.

In conclusion, NG neurons form a previously unknown network of electrically and chemically connected neurons in the hippocampus that are well placed to modulate input into the CA1 from the perforant pathway.

We would like to thank Drs. Bruno Cauli and Bertrand Lambolez for providing PCR data, Drs. Akos Kulik and Ryuichi Shigemoto for ultrastructural analysis.

Where applicable, the experiments described here conform with Physiological Society ethical requirements.

C50

Synaptic integration in hilar mossy cells in the rat hippocampus in vitro

A.M. Thomas and M. Capogna

MRC, Anatomical Neuropharmacology Unit, Oxford, UK

The loss of hilar mossy cells (MC) is a common feature observed in the epileptic hippocampus, but despite a wealth of pathological data many physiological properties of MCs in the normal brain have still not been characterised. We have investigated if strong excitatory inputs from granule cells, intrinsic MC characteristics, either weak inhibition and/or integration favouring excitation can contribute to MC vulnerability.
Rats (13-24 days old) were humanely killed by decapitation and the brain removed, and hippocampal acute slices or slice cultures were prepared. Using biocytin labelling, minimal stimulation and paired recordings, we have selectively activated individual excitatory and/or inhibitory inputs onto MCs and studied MC-evoked excitatory currents in dentate granule cells.
Mossy cells were identified by the location of the soma, the presence of thorny excrescences on proximal dendrites and the pattern of axonal and dendritic arborisation, as visualised with light microscopy. MCs (n=15) displayed a characteristically large capacitance (215.40pF±15.83, mean±SEM), a sag in response to hyperpolarizing pulses (ratio=0.96±0.00), had a resting membrane potential of −62.71mV±2.03 and a membrane time constant of 49.67ms±2.65.
Minimal stimulation within the granule cell layer (n=10) of acute slices evoked all-or-none unitary IPSCs in MCs, with amplitudes of 48.00pA±6.72, rise times of 0.60ms±0.05, decay profiles that were better fitted by a single exponential (τ=10.10ms±1.04). IPSCs were abolished by the $GABA_A$ antagonist SR-95531 (1.2μM). Trains of stimuli, applied for 25ms at 40Hz, induced short-term depression of the IPSC (10th/1st IPSC=0.40±0.03). Conversely, minimal stimulation of granule cells evoked unitary EPSCs in MCs that facilitated when trains of 40Hz were applied and were inhibited by application of the group II metabotropic glutamate receptor (mGluRII) agonist, LY354740 (0.5μM).
Paired recordings in slice cultures revealed that granule cells evoked large, monosynaptic EPSCs in MCs (173.88±82.97pA, n=5). These EPSCs displayed paired pulse facilitation in control conditions and were inhibited by application of LY354740 (0.5μM), whereupon an increase in failures was always observed. Furthermore, granule cell firing frequently entrained MCs. Paired recordings further demonstrated that MCs evoked much smaller (20.06±5.66pA, n=7) monosynaptic EPSCs in granule cells that tended to display paired-pulse depression.
We conclude that hilar mossy cells receive strong and facilitating mossy fiber-mediated unitary EPSCs and short-term depressing unitary IPSCs.

Supported by the MRC.

Where applicable, the experiments described here conform with Physiological Society ethical requirements.

C51

Characterisation of layer VI cortical neurons activated by stimulation of callosal fibers

T. Karayannis and M. Capogna

MRC, Anatomical Neuropharmacology Unit, Oxford, UK

The great majority of callosal fibers are glutamatergic and excitatory. Anatomical studies have shown that during development almost 20% (0.7-5% in adult) of the fibers are GABAergic (Riederer et al 2004). However, functional properties of GABAergic neurons involved in the callosal-cortical circuits are unknown. Our aim is to elucidate the role of layer VI neurons, including GABAergic interneurons, in the callosal-cortical network.
Rats (14 to 24 days-old) were deeply anaesthetized using isoflurane, humanely killed by decapitated, and coronal acute slices, containing bilateral retrosplenial agranular (RSA) cortex and interhemispheric callosal fibers, were prepared. Whole-cell patch-clamp recordings were performed with pipettes containing K-gluconate and biocytin to reconstruct cellular morphology.
Electrical stimulation of the corpus callosum evoked heterogeneous synaptic responses recorded in voltage-clamp. Inward currents were evoked at −65mV with the following features: 20-80% rise time=0.39-2.05ms, decay=0.67-5.94ms, latency=4-9.4ms (n=20), and were blocked by the AMPA/kainate antagonist 6,7-dinitro-quinoxaline-2,3-dione (DNQX, 20 μM). Two cells responded with outward currents only, evoked at −50mV. The currents blocked by the $GABA_A$ antagonist SR95531 (4 μM), and three cells with inward/outward currents sequence. The EPSCs and IPSCs were likely to be monosynaptic, since they had low jitter (range: 0.11-0.73ms), and did not display failures.
With Cs^+-based pipette solution, a slower NMDA receptor-mediated EPSC was detected in the presence of 0.5μM DNQX and 0.5μM SR95531, with a maximum amplitude at −10mV, that was abolished by 40μM AP5. Furthermore, stimulation of the callosal fibers also evoked back-propagating action potentials when neurons sending axons through the corpus callosum were recorded (n=14).
Importantly, most of the recorded cells had intrinsic membrane properties and anatomical features indicative of GABAergic interneurons. Anatomically reconstructed cells had an interneuron-like shape with a small fusiform, bipolar soma, one apical dendrite and few dendritic branches. The cell firing was quite heterogeneous, often typical of cortical GABAergic interneurons (Gupta et al, 2003), consisting of fast-spiking accomodating and non-accomodating neurons, as well as stuttering types. We also recorded from regular spiking layer V-VI pyramidal cells, where stimulation of the callosal fibers evoked EPSCs with slower kinetics (range: 20-80%rise time=1.43-2.83ms, decay=10.17-18.9ms, latency=6-8.8ms, n=3).

Our data suggest that putative GABAergic interneurones are directly involved in the callosal-cortical network.

Riederer BM et. al. (2004) Eur J Neurosci 19, 2039-2046.
Gupta A et al. (2003) Science 287, 273-278.

Supported by MRC

Where applicable, the experiments described here conform with Physiological Society ethical requirements.

C52

Unitary purinergic excitatory synaptic currents in the pyramidal neurons of rat somatosensory cortex

Y. Pankratov and A. North

Faculty of Life Science, The University of Manchester, Manchester, UK

Spontaneous excitatory postsynaptic currents (sEPSC) were recorded in neocortical rat pyramidal neurones in vitro using conventional whole-cell voltage clamp technique, in the presence of tetrodotoxin (TTX: 10 μM) and picrotoxin (100 μM). Experiments were carried out on transverse 280-300 μm thick slices of CBL57 mice (15- to 45-day-old) brain. The animals were humanly killed. Application of glutamate receptors antagonists 6-cyano-7-nitroquinoxaline-2,3-dione (CNQX: 50 μM) and D(-)-2-amino-5-phosphonopentanoic acid (D-APV: 30 μM) led to a significant but not complete reduction of sEPSC amplitude. The residual sEPSCs (rsEPSCs) were not affected by combined application of (2S,4R)-4-methylglutamic acid (SYM2081: 10 μM, to desensitize kainate receptors) and (RS)-4-(4-aminophenyl)-1,2-dihydro-1-methyl-2-propylcarbamoyl-6,7-methylenedioxyphthalazine (SYM2206: 50 μM, a non-competitive AMPA receptor antagonist). This suggests that rsEPSCs are mediated neither by AMPA/kainate nor by NMDA receptors. The amplitude of the rsEPSC was 67 ± 15% (mean ± SD, n = 41) of the control sEPSC, and the frequency of residual synaptic events was 39 ± 20% (n = 41) of control. The rsEPSCs were not affected by the nicotinic receptors antagonist hexamethonium (100 μM) or the adenosine A1 receptor antagonist 8-cyclopentyl-1,3-dipropylxanthine (DPCPX: 1 μM). They were inhibited by P2X receptors antagonists pyridoxal-phosphate-6-azophenyl-2',4'-disulfonate (PPADS:10 μM) and 8,8'-[carbonylbis(imino-4,1-phenylenecarbonylimino-4,1-phenylenecarbonylimino)]bis-1,3,5-naphthalenetrisulfonic acid (NF279: 1 μM). The amplitude distribution of synaptic currents in control conditions showed two distinct peaks. The major peak with higher amplitude disappeared after application of CNQX. The minor peak was not altered by glutamate receptor antagonists, but was shifted towards lower amplitudes by PPADS and suramin. Although there was no large difference in the kinetics of sEPSC before and after CNQX, a difference was revealed by cyclothiazide (CTZ). Application of CTZ (50 μM) did not alter the kinetics of the synaptic current recorded in CNQX (decay time 10 ± 2 ms, n=8), whereas the decay time of current recorded in the presence of suramin (10 μM) increased more than two-fold (decay time 19 ± 3 ms, n=5). The distribution of decay times of the sEPSC was unimodal in control conditions, but became bimodal in CTZ with the major peak increased two-fold. The above results suggest the existence of distinct population of purinergic synaptic events which occur asynchronously with respect to those mediated by glutamate. Although the probability of unitary ATP-mediated synaptic events is much lower, their amplitude is comparable to the amplitude of glutamate-mediated events. This may imply a specific role for the purinergic component of excitatory synaptic transmission

Where applicable, the experiments described here conform with Physiological Society ethical requirements.

C53

Sub-millisecond synchronization of spike activity in the Isthmi nuclei of pigeons (*Columba livia*)

G. Marin, J.C. Letelier, E. Sentis, H.R. Maturana and J. Mpodozis

Biology, Universidad de Chile, Santiago, Chile

Brief periods of fast oscillations are prominent components of the sensory-evoked potential recorded in the cortex and thalamus of anesthetized and awake animals (Barth, 2003), including humans (Curio, 2000). Consistent evidence indicates that these fast oscillations reflect the synchronized firing of local neural elements. However, how this synchronization is brought about and what exactly is the biophysical correlate of fast oscillations have been matters of intense discussion. It is generally accepted that high frequency synchronization is confined to small neuronal space (Buzsaki & Draguhn, 2004). In this study, by recording in the isthmi nuclei of the pigeon, we show that a confined, high frequency synchrony event can spread to a larger neuronal surface by an organized divergent efferent projection.

The nucleus isthmo pars parvocellularis (Ipc) and the nucleus isthmo pars magnocellularis (Imc) are laminar structures reciprocally connected to the optic tectum. Imc neurons, presumably GABAergic, also project to Ipc with widely ramified axonal fields covering most of the nucleus (Wang et al. 2004a). The isthmi constitute a neural loop that modulates the visual responses of tectal cells (Wang et al. 2004b).

We recorded neuronal activity in Ipc and Imc in response to flashing and visual motion stimulation. We did single and dual microelectrode recordings using tungsten and fine pipettes in anesthetized pigeons (ketamine/xylazine, 5/50 mg/kg, i.m.; anaesthesia was maintained by supplementary doses every 2 h). Ipc neurons responded with trains of high frequency bursts to visual stimulation presented in a 15-20 deg excitatory receptive field (RF). In addition to this response, in every Ipc recording loci, visual stimulation of discrete regions outside the RF elicited a high frequency, 600 Hz, negative wave of variable amplitude (100-400 μV). Recording from two widely separated regions (0.7-1 mm) in Ipc revealed that, while each region has a distinct excitatory RF, both regions share the locations in visual space from where this high frequency oscillation was elicited. Notably, the oscillations recorded from both electrodes almost totally overlapped. Intracellular staining with biocytin, demonstrated that Imc neurons and Imc terminals in Ipc, with RFs overlapping these visual regions, fired in high frequency barrages phase-locked to this wave. These results indicate that a local ensamble of Imc neurons can get sinchronized in the sub-millisecond range and induce a phase locked oscillation in their terminal fields through-

out Ipc. Consequently, separated regions in Ipc would receive a common input drive synchronized at the same timescale.

Barth DS (2003). J Neurosci **23,**, 2502-2510
Curio G (2000). J Clin Neurophysiol **17,**, 377-396
Buzsaki G & Draguhn A (2004) Science **304,**, 1926-1929
Wang Y et. al. (2004a) J Comp Neurol **469,**, 275-297
Wang Y et. al. (2004b) J Comp Physiol A **186,**, 505-511

Supported by Fondecyt no. 1030522

Where applicable, the experiments described here conform with Physiological Society ethical requirements.

C54

Burst stimulation alters the excitability of hypothalamic axons

R.E. Dyball and A.N. Inyushkin

Anatomy, University of Cambridge, Cambridge, UK

We recently reported that the entropy of the log interspike interval distribution recorded from hypothalamic neurones changes in response to physiological stimuli (Bhumbra & Dyball, 2004). It is thus important to know if subtle changes in interval distribution might have physiological significance. Dyball & McKenzie (2000) showed that the excitability of axons in magnocellular neurosecretory neurons of the supraoptic nucleus changes during trains of applied stimuli. There is an input to the arcuate nucleus (ARCN) from the suprachiasmatic nucleus (SCN). We thus examined whether short bursts of stimuli applied to the ARCN region that evoked antidromic action potentials in SCN cells might alter the excitability of their axons.

Extracellular recordings were made from the suprachiasmatic nucleus (SCN) in 500 μm sagittal brain slices from Wistar rats and C57 black mice. All animals were humanely killed. Recordings were made from SCN cells that were antidromically activated from the arcuate nucleus (ARCN). Trains of 20 just-subthreshold stimuli at 50 Hz repeated at 1 s intervals decreased the threshold for antidromic activation. Whereas neither single subthreshold stimuli nor stimuli at the beginning of a train of 20 pulses evoked antidromic action potentials, later stimuli in the train did so. To test whether the increased excitability was mediated by local changes in potassium ion concentration at the stimulus site, we progressively increased the concentration of potassium in the perfusion solution while continuously stimulating at 1 Hz with a constant, subthreshold, intensity. Increased potassium concentration increased the number of antidromically activated spikes suggesting an enhanced excitability. By contrast, trains of 20 just-suprathreshold stimuli increased the threshold for antidromic activation in SCN cells. Whereas single suprathreshold stimuli invariably evoked an antidromic action potential, identical stimuli applied in trains of 20 pulses failed to evoke spikes after a few stimuli. After the first train of 20 pulses, the later stimuli in the trains fell below threshold and antidromic action potentials were not evoked.

The decreased excitability of the SCN cells during train stimulation of the ARCN region may be due to a hyperpolarizing afterpotential. The increased excitability is however probably mediated by local changes in potassium concentration. Both increased and decreased excitability may be important if short bursts of spikes can alter the likelihood of their propagation to axon terminals and influence release of neurotransmitters and thus transmission at synapses.

GS Bhumbra & REJ Dyball (2004). J. Physiol. 555, 281-296.
Dyball REJ. & McKenzie DN (2000). J. Neuroendocrinol. 12, 729-735.

We thank the EPSRC for financial support.

Where applicable, the experiments described here conform with Physiological Society ethical requirements.

C56

Calcitonin gene-related peptide induced suppression of LH pulses in the rat: the role of endogenous opioid peptides

J. Bowe[1], X. Li[1], J. Kinsey-Jones[1], S. Paterson[3], S. Brain[2] and K. O'Byrne[1]

[1]Division of Reproductive Health, Endocrinology and Development, King's College London, London, UK, [2]Centre for Cardiovascular Biology, King's College London, London, UK and [3]Neuroscience Research, King's College London, London, UK

Calcitonin gene-related peptide (CGRP) is involved in a variety of stress responses in the rat. Central administration of CGRP activates the hypothalamo-pituitary-adrenal axis, specially enhancing corticosterone release. We have previously shown that central CGRP suppresses the gonadotropin-releasing hormone (GnRH) pulse generator, specifically LH pulses. Endogenous opioid peptides (EOP) have been shown to play an important role in stress-induced suppression of the reproductive axis and are additionally involved in various CGRP effects within the brain. The aim of the present study was to test the hypothesis that EOP mediate CGRP-induced suppression of pulsatile LH secretion.

Wistar rats, anaesthetized with ketamine (100 mg kg^{-1}, ip) were ovariectomized and chronically implanted with intracerebroventricular (icv) and intravenous (iv) cannulae (ketamine, 100 mg kg^{-1}, ip). Blood samples (25μl) were collected at 5 min intervals for 6hrs for the detection of LH by radioimmunoassay. After 2 h CGRP (1.5 or 5μg/4μl) was administred icv either alone, or in addition to naloxone (250μg/200μl), given iv 10 min prior to CGRP injection (n=7-12). Additionally 1.5μg CGRP icv was co-administered after 2hr with naloxone (10μg icv), norbinaltorphimine (nor-BNI, 5μg icv) or naltrindole (5μg icv), μ, κ and δ specific opioid receptor antagonists respectively (n=6-8). Controls received 4μl icv of artificial cerebrospinal fluid.

The 1.5μg icv infusion of CGRP significantly (paired Student's t test, $p<0.05$) prolonged the LH inter-pulse interval from 29.3±3.4 min (mean±sem) before treatment to 38.7±4.6 min after treatment (n=12). The higher dose (5μg CGRP) completely abolished LH pulses for the duration of the 4 h post-treatment period (n=8). Naloxone (250μg iv) completely blocked the inhibitory effects of 1.5μg CGRP on LH pulses in all rats treated, and significantly (paired Student's t test, $p<0.05$)attenuated the effects of 5μg CGRP. Co-administration of icv naloxone or nor-BNI completely blocked the inhibitory effects of 1.5μg CGRP on LH pulses whilst naltrindole did not.

These data provide evidence that EOP play a pivotal role in mediating the inhibitory effects of CGRP on pulsatile LH secretion in the rat. The data also shows that the μ and κ, but not the δ,

specific opioid receptors, are responsible for mediating the effects of CGRP on LH pulses.

This work was supported by the Guy's & St Thomas's Charitable Foundation and Wellcome Trust.

Where applicable, the experiments described here conform with Physiological Society ethical requirements.

C57

Glucosensing neurons are present in the rat brainstem and express glucokinase

R.H. Balfour[1], A. Kruse Hansen[2] and S. Trapp[1]

[1]Department of Anaesthetics & Intensive Care, Imperial College, London, UK and [2]Research & Development, Novo Nordisk A/S, Maaloev, Denmark

Homeostatic control of brain glucose involves the hypothalamus and lower brainstem. We have identified and characterised glucosensing neurons in the vagal complex of the brainstem using *in situ* hybridisation, single-cell RT-PCR and whole-cell patch-clamp recordings from 200 μm thick brain slices.
Slices were obtained from juvenile Sprague-Dawley rats humanely killed following halothane anaesthesia. After 30 min recovery at 34°C slices were kept at 22°C in artificial cerebrospinal fluid (ACSF). Whole-cell recordings from 153 cells were performed under visual control. From 30 cells cytoplasm was aspirated into the electrode after patch-clamp recording and used for single-cell RT-PCR. *In situ* hybridisation was performed with biotin-labelled riboprobes for glucokinase (GLK) on 30μm coronal brainstem sections cut from perfuse-fixed tissue on a cryostat. Results were visualised with an avidin-alkaline phosphatase conjugate and BCIP/NBT colour substrate. To identify glia, slices were also incubated with an anti-GFAP (glial fibrillary acidic protein) Cy3-conjugate.
Hypoglycemic responses of neurons in the dorsal vagal nucleus and the nucleus tractus solitarius were tested by a change from 10mM to 0mM ACSF glucose. Most neurons did not respond to this challenge within 5min (non-responsive: NR). 15 neurons tested depolarised from -59±2 mV within 155±31s (mean±s.e.m) of glucose removal (glucose-inhibited: GI). 11 hyperpolarised by 14±2mV and stopped firing within 53±7s (glucose-excited: GE). The hyperpolarisation was reversed by 10mM glucose or 100μM tolbutamide, a K_{ATP} channel blocker. Single cell RT-PCR showed that all GI (n=3), 2 of 3 GE, and 0 NR (n=24) expressed GLK. 1 GI, the 2 GLK-positive GE and 11 NR also expressed SUR1, a K_{ATP} channel subunit.
In situ hybridisation revealed widespread staining for GLK across the lower brainstem (n=7). In the vagal complex strongly stained cells were found in the dorsal vagal nucleus, nucleus tractus solitarius and area postrema. Glucokinase was not co-localised with GFAP (n=4), suggesting that glucosensors are primarily neuronal. We have demonstrated that GI and GE neurons exist in the brainstem and suggest that GLK is essential for their function. GE cells work analogous to pancreatic β-cells requiring both GLK and K_{ATP} channels. Vagal glucosensors might be involved in the regulation of vagal outflow to the pancreas providing CNS influence on blood glucose levels dependent on brain glucose availability.

This work was supported by an MRC Career Development Award to ST

Where applicable, the experiments described here conform with Physiological Society ethical requirements.

C58

Glutamate mediates rapid glucose transport inhibition in neurons and stimulation in astrocytes as evidenced by real-time confocal microscopy

O. Porras[1], A. Loaiza[2] and F. Barros[1]

[1]Biofisica y Fisiologia Molecular, Centro de Estudios Cientificos, CECS, Valdivia, Chile and [2]Universidad Austral de Chile, UACH, Valdivia, Chile

It is known that brain activity is fueled by glucose, but the identity of the cell type that metabolises the sugar remains elusive. In order to address the issue, we have developed transport assays that allow single-cell real-time measurement of glucose transport in mixed rat hippocampal cultures using confocal microscopy. Our data shows that the neurotransmitter glutamate triggers opposite responses in astrocytes and neurons. Astrocytes, which only express GLUT1, responded with a two to three-fold stimulation of the uptake rate of the hexoses 6-NBDG, 2-NBDG and galactose. The effect was due an increase in the Vmax for uptake. The rate of efflux was unaffected, which using the ″simple carrier″ model can be accounted economically by a decrease in the asymmetry of the transporter. Strikingly, neurons responded with a > 80% inhibition of the hexose uptake rate. The IC50 was 5 μM, which is well in the range estimated for glutamate in the synaptic cleft. The phenomenon in neurons was mimicked by AMPA and was abolished pharmacologically by CNQX and functionally by removal of extracellular sodium, so it is seems to be mediated by AMPA receptors. Both astrocytic stimulation and neuronal inhibition of hexose uptake rates by glutamate were detected in the range of seconds and reverted upon glutamate removal We conclude that glutamate redistributes glucose towards astrocytes and away from neurons. These phenomena provide novel regulatory nodes for brain energy metabolism and support a model in which blood-borne glucose is first metabolised by astrocytes and then transferred to active neurons as a more oxidized form, perhaps lactate. Were these mechanisms to be functional in the brain, they would mean that functional imaging by FDG-PET scanning reports an astrocytic phenomenon, although directly linked to neuronal activity by means of glutamate release.

This work was funded by FONDECYT 1020648. Institutional support to the Centro de Estudios Cientificos (CECS) from Empresas Companias Manufactureras de Papeles y Cartones.

Where applicable, the experiments described here conform with Physiological Society ethical requirements.

C59

The glial NH_4^+ -Cl^- cotransporter facilitates the neuron-glia ammonium flux in bee retinae

J.A. Coles

Université Joseph Fourier/INSERM U594, Grenoble, France

Expression of mRNA coding for putative ammonium transporters is widespread, but the functions of ammonium transporters have been little studied except in plant roots and kidneys (Ludwig et al, 2004). Glial cells of the compound eye of the bee take up $NH4^+$ by cotransport with Cl^- (Marcaggi & Coles, 2000). It has been proposed that the neurons of bee retina (which are all photoreceptors) are provided by the glial cells with alanine as their major energy substrate (Tsacopoulos et al, 1994). Conversion of alanine to pyruvate releases ammonium, which may return to the glial cells. To test this proposal, I used ion-selective microelectrodes to measure $[NH_4^+]$ in the interstitium of slices of drone retina superfused with (mM) NaCl, 205; KCl, 10; $MgCl_2$, 4; $CaCl_2$, 2; MOPS, 10; sucrose, 240; pH 6.90. One barrel of the electrode contained an "ammonium" sensor sensitive to both NH_4^+ and K^+(Bührer et al 1988), one barrel contained a K^+ sensor based on valinomycin, and the third barrel measured the electrical potential; the total tip diameter was 3 - 4 μm. When the photoreceptors were stimulated with a train of light flashes, there was a large K^+ signal: to extract the much smaller NH_4^+ signal, I calibrated the electrode immediately after any measurement (Fig. 1). With the standard superfusate solution, interstitial $[NH_4^+]$ was not detected even at the end of 120s light stimulation (mean, 0.072 mM; SEM, 0.091 mM, n = 9). When superfusate Cl^- was replaced by glucuronate and gluconate, interstitial $[NH_4^+]$ was detectable: 0.290 ± 0.089 mM (n = 10; P by Student's t test < 0.01) in the dark; 0.41± 0.12 mM after 120s light stimulation (n = 9). Since removal of Cl^- blocks uptake of NH_4^+ into the glial cells, these results suggest that the NH_4^+-Cl^- cotransporter normally aids the flow of ammonium from the neurons to the glia. Inclusion of 25 mM alanine in the superfusate significantly reduced the variance of the $[NH_4^+]$ measurements (P = 0.0009 with Cl^-, and P = 0.011 without) but did not change the mean values. When 10 mM Na pyruvate was substituted for 10 mM Na glucuronate in the 0 Cl^- superfusate, $[NH_4^+]$ at the end of the stimulation was reduced to 0.04±0.10 mM (n = 5, P < 0.002) apparently without loss of neuronal function.

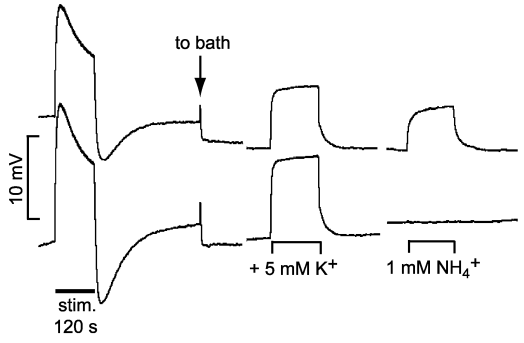

Fig. 1 Potentials (reference subtracted) of the "ammonium" barrel (top), and the K barrel (bottom) in a slice superfused with 0 Cl^- solution. Light stimulation for 120s transiently increased both signals. The electrode was then calibrated in 0 Cl^- solutions, responses to two solutions being shown. The gaps in the record correspond to 1.75 and 1.35 ks.

Bührer *et al* (1988) *Pflügers Arch***412**, 359-3624.

Ludewig U (2004). *J Physiol* **559**, 751-759.

Marcaggi P & Coles JA (2000) *J Gen Physiol* **116**, 125-141.

Tsacopoulos M *et al* (1994) *J Neurosci* **14**, 1339-1351.

Where applicable, the experiments described here conform with Physiological Society ethical requirements.

C61

Alcohol Induced Motor Impairment Caused by Increased Extrasynaptic $GABA_A$ Receptor Activity

P.D. Dodson[1], M. Wallner[2], H.J. Hanchar[2], R.W. Olsen[2] and T.S. Otis[1]

[1]Department of Neurobiology, University of California, Los Angeles, Los Angeles, CA, USA and [2]Department of Molecular and Medical Pharmacology, University of California, Los Angeles, Los Angeles, CA, USA

Molecular targets for the actions of behaviourally relevant concentrations of alcohol remain elusive. We have identified a class of $GABA_A$ receptors, found in extrasynaptic membranes, which are sensitive to alcohol concentrations achieved after consumption of one drink. One type of these receptors ($\alpha6\beta3\delta$) is only expressed in cerebellar granule cells where it generates a form of tonic inhibition. We report that low concentrations of alcohol act at these receptors, causing motor impairment.

We examined the effects of ethanol on Sprague-Dawley rats bred to be homozygous either for the wild type ($\alpha6^{100R}$) or for mutant ($\alpha6^{100Q}$) alleles of a point mutation thought to enhance the alcohol sensitivity of α6 containing GABA receptors; we then used the mutant animals as a tool to investigate the behavioural actions of alcohol at these receptors. We made whole-cell recordings from granule cells in 300μm parasagittal cerebellar slices from humanely killed P24-42 Sprague-Dawley rats. Cells were clamped at -70 mV using CsCl containing pipettes. Homozygous rats (>P55) were tested on an accelerating rotarod test in which the speed of rotation was increased at a constant rate from 4 to 40 rpm over 5 minutes. Data are presented as mean ± S.E.M. Statistical significance was assessed with Student's t tests or a Wilk's lambda multivariate test.

Tonic GABA conductance in granule cells from both genotypes was sensitive to concentrations of ethanol as low as 10 mM. 30 mM ethanol increased the tonic conductance by 15.7 ± 2.5% (n=5) in wild type granule cells and caused a significantly larger increase (68 ± 11.1%, n=7, P<0.01) in those from $\alpha6^{100Q/Q}$ rats. Moreover mutant animals showed greater motor impairment in response to low doses of ethanol than wild types (P<0.01) n=6 and 7 respectively). 20 minutes after intraperitoneal injection of low doses of ethanol (1g/kg) wild type rats showed only mild motor impairment (the average time that they were able to stay on the rotarod was reduced by 13.1 ± 5.2%, n=6) whereas mutant $\alpha6^{100Q/Q}$ rats were significantly more impaired (27.9 ± 3.6% n=6, P<0.03), suggesting that ethanol enhancement of granule cell tonic inhibition is responsible for alcohol-induced motor impairment. These findings not only identify extrasynaptic $GABA_A$ receptors as a primary alcohol target but also that action at these receptors can account for the effects of alcohol on motor function.

This work was supported by a Human Frontiers Science Program Long-Term Fellowship to P.D.D., NIH grants NS40499 to T.S.O., NS35985 and AA07680 to R.W.O.

Where applicable, the experiments described here conform with Physiological Society ethical requirements.

C62

Calmodulin regulation of exocytosis in bovine adrenal chromaffin cells

R. Wykes and E. Seward

Department of Biomedical Sciences, University of Sheffield, Sheffield, UK

We have previously reported that calmodulin (CaM) acts directly to control N-type calcium channel inactivation in cultured bovine adrenal chromaffin cells (Wykes & Seward, 2004). Here we report that CaM additionally interacts with the secretory machinery to regulate exocytosis. Stimulus-secretion coupling was examined in single cells using combined measurements of membrane capacitance (ΔCm) and voltage-clamp recording of calcium currents. Cells were clamped at -80 mV in either the perforated patch or whole-cell configuration and Ca^{2+} dependent exocytosis evoked by single voltage steps to +20 mV or a train of depolarisations (10-100ms duration); exocytotic efficiency was derived by dividing ΔCm by the integral of the calcium current. Adenoviral-mediated expression of a mutant CaM incapable of binding calcium (CaM1234) significantly reduced the exocytotic efficiency of brief depolarisations (100 ms) to 0.30 ± 0.03, n=7, from 0.75 ± 0.16, n=5 ($p = 0.0008$, Student's t test) in cells overexpressing wild type CaM (CaM_{wt}). The exocytotic efficiency to longer depolarisations (≥ 200ms) however was not significantly different between cells expressing CaM_{1234} and CaM_{wt}. This suggests that Ca^{2+}-CaM is required for filling and/or release from a rapidly releasable pool of vesicles which is easily depleted, but not from the slowly releasable pool which dominates exocytotic responses measured with prolonged responses. A protocol designed to look at different releasable pools of vesicles (a train of 6, 10ms pulses, followed by 4, 100ms pulses to +20 mV) confirmed this observation. With this protocol, the 10ms stimuli will result in a ΔCm that reflects fusion from the immediately releasable vesicle pool, while the further 4 longer pulses result in a second bout of secretion dominated by release from the slowly releasable vesicle pool (Voets, 2000). CaM1234 expression reduced the size of the immediately releasable vesicle pool, quantified by measuring responses to a pair of 10 ms depolarisations, to 14 ± 5 fF, n=18, corresponding to ~ 7 vesicles compared with 58 ± 17 fF, n = 15 or 29 vesicles in cells overexpressing CaM_{wt}, $p = 0.01$. Taken together, these results place CaM as a central molecule that controls Ca^{2+} entry (Ca^{2+} channels) and the exocytotic and endocytotic machinery to regulate stimulus-coupled secretion. Primary cultures of bovine chromaffin cells were made weekly from glands collected from a local abattoir.

Wykes R.C. and Seward E.P., 2004, J Physiol. 557P.

Voets T., 2000, Neuron 28:537-545.

Where applicable, the experiments described here conform with Physiological Society ethical requirements.

C63

Experience-dependent potentiation of *Drosophila* neuromuscular junctions is mediated by presynaptic NMDA receptors

J.R. Steinert and C.M. Schuster

Neurobiology, ICN, Heidelberg, Germany

The developing neuromuscular junction (NMJ) of *Drosophila* larvae is used as a simple model for genetic analysis and activity-dependent processes at glutamatergic synapses. However, due to the mostly chronic effects caused by mutations, little is known in this system about acute experience-dependent regulation of synaptic performance. We therefore used a newly developed behavioural assay (1) to stimulate NMJs by enhanced larval locomotor activity to characterise the first two hours of experience-dependent potentiation of signal transmission. Intracellular recordings of *Drosophila* larvae muscle 6 were performed in bridge mode and two-electrode voltage clamp (AxoClamp 2B, Axon Instruments) in haemolymph-like solution 3 solution. Data are expressed for miniature excitatory potentials (mEJP) or evoked excitatory potentials/currents (eEJP/eEJC) as mean±S.E.M., where n indicates the number of different larvae. Statistical analyses were carried out using ordinary ANOVA where applicable and a two-tailed Student's t test for unpaired or paired data. *P<0.05 considered statistically significant.

We show that after resting signal transmission (lag-phase [0-35min], mEJP: 0.98±0.07mV, n=19, eEJP: 40.5±1.8mV, n=19) experience-dependent activation of the NMJ led initially to enhanced mEJP and eEJP amplitudes during a transient phase which was driven by the release of large presynaptic quanta of glutamate (phase I [35-85min], mEJP: 1.70±0.08mV*, n=33, eEJP: 50.3±1.5mV*, n=20). This period was followed by a second phase (phase II [90-120min], mEJP: 1.05±0.08mV, n=16, eEJP: 51.6±0.9mV*, n=13) which was sensitive to specific NMDA receptor (NMDAR) antagonists. Furthermore, when analysing postsynaptic decay kinetics of eEJCs we found no change during phase II (lag-phase: τ=3.8±0.1ms, n=4 *vs* phase II: τ=3.0±0.3ms, n=4) nor after application of APV (NMDAR antagonist) in phase II (τ=2.9±0.5ms, n=3), indicating that NMDARs with typical decay kinetics are not postsynaptically active. To prove the presence of presynaptic *Drosophila* NMDARs (DNMDARs) we expressed dominant negative or wild type DNMDAR constructs post- and presynaptically, with only the expression of dominant negative DNMDARs in motorneurons eliminating the APV-sensitive component of potentiation in phase II reinforcing that previously unidentified presynaptic DNMDARs are responsible for the experience-dependent potentiation in phase II. By defining the two mechanistically distinct phases this study offers new insights into the mechanisms mediating the first two hours of experience-dependent potentiation of glutamatergic signal transmission.

(1) J.R.Steinert, A.W.Wyatt, J.Wismar, B.Schmitt & C.M. Schuster (2004) submitted MS

This work was supported by Deutsche Forschungsgemeinschaft.

Where applicable, the experiments described here conform with Physiological Society ethical requirements.

PC58

Characterization of nicotine acetylcholine receptors in cultured cat petrosal ganglion neurones

V. Valdes[1], R. Iturriaga[2] and J. Alcayaga[3]

[1]Fisiologia, Pontificia Universidad Catolica de Chile, Santiago, Chile, [2]Fisiologia, Pontificia Universidad Catolica de Chile, Santiago, Chile and [3]Biologia, Facultad de Ciencias, Universidad de Chile, Santiago, Chile

The petrosal ganglion (PG) neurones that innervate the carotid body, through the carotid sinus nerve, respond to exogenously applied ACh. About 60% of PG neurones in culture respond to ACh with dose-dependent inward currents, depolarization and action potentials, effects mimicked by nicotine and blocked by hexamethonium and mecamylamine. However, little is know about the identity of this nAChR. Immunohistochemical studies revealed that α7 and α4 nAChR subunits are present in the nerve endings and in the perikarya of cat PG neurones. To further characterize the receptors involved in PG neurones response to ACh, we studied the responses elicited in isolated petrosal ganglion neurones by selective agonists and antagonists of nAChRs.

PG neurones were obtained from 10 adult cats anesthetized with pentobarbitone (40 mg kg^{-1} i.p.). Animals were killed by an overdose of pentobarbitone. The cells were enzymatically dissociated, plated in Petri dishes and maintained at 38°C in water-saturated, 5% CO_2 in air atmosphere. The experimental protocol was approved by the Ethical Committees of both Faculties and met the guidelines of the Chilean National Fund for Scientific and Technological Development (FONDECYT). The currents evoked by ACh, cytisine (an alkaloid with micromolar affinity for α7 homomeric nAChRs) and its brome derivatives, 3-bromecytisine (3Br-cytisine; a selective agonist of α7 homomeric nAChRs), and 5-bromecytisine (5Br-cytisine; a selective agonist of α4β4 nAChRs), were measured using whole-cell voltage-clamp recordings at a holding potential of −60 mV. The agonists and antagonists, hexamethonium and α-bungarotoxin, were applied by superfusion under gravity from a pipette near the neurone surface. Pooled data of individual cells were fitted to a logistic curve [$I = Imax/1+ (EC_{50}/X)^n$], yielding correlation coefficients higher than 0.90 ($p < 0.01$) for all conditions studied.

ACh evoked a fast inactivating inward current, whose amplitude showed a dose-dependent increase and was reversibly blocked by 1 μM hexamethonium. The ACh-sensitive neurones (10/16), also responded to cytisine, 3Br-cytisine and 5Br-cytisine with fast inactivating inward currents. The potency order of the agonists, according to their EC_{50}, was 3Br-cytisine >> ACh ≅ cytisine > 5Br-cytisine. Furthermore, 10 nM α-bungarotoxin blocked the responses induce by ACh in 5 out of 6 neurones, which electrical properties remained unchanged during the application of the antagonist. Our results suggest that most PG neurones respond to ACh by the activation of α7 nAChRs.

Work supported by grants FONDECYT 1040638, 1030330 and 1010951

Where applicable, the experiments described here conform with Physiological Society ethical requirements.

PC59

Altered redox-status modifies excitability in mouse cultured spinal cord neurones

U.V. Boolaky[1], D.M. Bailey[2] and K.T. Wann[1]

[1]Welsh School of Pharmacy, Cardiff University, Cardiff, South Glamorgan, UK and [2]Departments of Anesthesiology and Surgery, University of Colorado Health Sciences Center, Denver, CO, USA

Oxidative stress (OS) is implicated in Amyotrophic Lateral Sclerosis (ALS), a progressive and fatal neurodegenerative disease (Cookson and Shaw, 1999). The present study was designed to assess the functional changes in motor neurones (MNs) following exposure to OS using cell-attached patches to measure the effects of H_2O_2 on both cellular excitability and single channel activity. Spinal cord cultures were grown from humanely killed E13 mice (Boolaky et al. 2002), MNs being identified morphologically and immunohistochemically. Whole-cell and cell-attached recordings were made. The bath solution contained (mM): 140 NaCl; 3 KCl; 2 $MgCl_2$; 2 $CaCl_2$; 10 HEPES; 10 Glucose, pH 7.4. The pipette solution contained (mM): 140 KCl; 5 NaCl; 1 $MgCl_2$; 1 $CaCl_2$; EGTA 11; HEPES 10, pH 7.2. In single-channel experiments 1 μM TTX was added to the bath solution. Cells were patched under control conditions and following incubation for 1 hour (5% CO_2, 37°C) in medium containing 100μM H_2O_2. All recordings were made at 0mV pipette potential (pp). Electron paramagnetic resonance (EPR) spectroscopic detection of α-phenyl-tert-butylnitrone adducts was incorporated for direct detection of free radicals.

Control cells possessed healthy RMP, and 88 % of cells had spontaneous biphasic action currents. Following treatment with 100μM H_2O_2, both the RMP (Table 1) and the number of cells firing decreased to 59%; the interspike interval, a measure of firing frequency, increased. The Popen of large conductance maxi-K channels, at 0mV pp, was significantly increased in MN (Table 1) and the voltage dependence was decreased following H_2O_2-treatment (n = 4). Incubation with 100μM riluzole did not prevent membrane depolarisation or the reduction in the firing frequency, although it did prevent reduction in the number of cells firing.

EPR spectroscopy showed that incubation with 100μM H_2O_2 increased the concentration of lipid-derived free radicals identified as a combination of alkoxyl, alkyl and hydroxyl radical species. However, this was not affected following addition of 100μM riluzole.

This study demonstrates that OS induced by H_2O_2 produces significant changes in the excitability of MN in culture. Such changes may mirror the excitability increases in ALS and underpin neurodegeneration

Table 1: H_2O_2 and MN excitability.

Conditions	Interspike interval (s) (mean±SEM)	RMP (mV)	Mean P_{open}
Controls	0.59 ±0.13 (n = 22)	-53.7 ±1.7 (n=7)	0.008±0.007 (n=12)
100μM H_2O_2	2.63±0.96 (n=3)*	-30.50 ±10 (n=6)*	0.165±0.08 (n=8)*
100μM H_2O_2 and 100μM riluzole	1.45±0.47 (n=9)*	-34.6±5 (n=7)	

***P ≤ 0.05 (independent Student's t test).**

Boolaky UV et al. (2002). Amyotroph Lateral Scler Other Motor Neuron Disord 3(S2): 80.

Cookson, M. R. & Shaw, P. J. (1999) Brain Pathol 9, 165-86.

Where applicable, the experiments described here conform with Physiological Society ethical requirements.

PC60

Structural change of GABAA receptors during early development in the visual cortex

B. Morales, C. Rozas, M. Encina, M. Zeise and F. Pancetti

Neuroscience Lab, Department of Biology, University of Santiago of Chile, Santiago, Chile

Experience induces profound functional and structural modifications in the visual cortex neuronal circuits. These modifications occurs in the early postnatal life, during a brief period of time called critical period. Long-term potentiation (LTP) and long-term depression (LTD) have been proposed as models by which this plasticity occur. Similar to the ocular dominance, the induction of LTP and LTD in rats have critical periods of around 5 weeks, however the cellular and molecular mechanisms that initiate and eventually end this critical period are still controversial. We show evidence that the maturation of GABAergic circuits, which also reaches a maximum in the 5th week, plays an important role in establishing the end of the critical period for the induction of synaptic plasticity in visual cortex. Slices of 300 μm thick were obtained from 3-8 week-old Long evans rats, killed by decapitation under halothane anesthesia according with the guidelines of the Ethics Committee of the University of Santiago, and maintained in artificial cerebrospinal fluid for 1 hr before recording. GABAergic whole cell currents evoked with protocols of 15 repetitive stimuli between 1 to 50 Hz, applied to layer 4, were recorded from layer 2/3 under symmetric Cl- conditions. Field post-synaptic excitatory potentials were evoked by electrical stimulation with bipolar electrodes localized on the white matter and recorded from layer 2/3. LTP or LTD were induced either after tetanic or low frequency stimulation, respectively. After the electrophysiological experiments, the slices were frozen and analyzed by inmunoblotting for the presence of GABAA receptor subunits. The results obtained at -80 mV in the presence of 20 μM CNQX and 100 μM APV to block fast glutamatergic transmission, show that IPSCs recorded in cells from 3 weeks old rats became depressed during the train. The peak response amplitude rapidly decreased, reaching a steady level by the 10th pulse. The maximal attenuation in pyramidal neurons from 5 week old rats (0.49±0.05%, n=14) was significantly smaller than in 3 week old animals (0.32±0.04%, n=12; Mann-Whitney U test, Z=-3.36, P<0.001). It was also observed that there is a decrease in the amplitude of LTP (Z=1.98, P<0.05) and LTD (Z=-1.96, P<0.05) that correlates with age, being easier to induce plasticity in 3 week old rats than in rats older than 5 weeks. Interestingly, we found that both effects are correlated with a structural change of the GABAA receptor during development. The expression of GABAA receptor ?2 subunit is higher in 3 week old than in 5, 6 and 8 weeks old rats. The evidence suggests that the GABAergic currents are important in establishing the critical period for plasticity in the visual cortex and this could be in part due to structural changes of the GABAA receptor subunits.

FONDECYT 1030220, DICYT-USACH Grants.

Where applicable, the experiments described here conform with Physiological Society ethical requirements.

PC62

Mitochondrial dysfunction in the hippocampus following status epilepticus: effects of levetiracetam

J.E. Gibbs and H.R. Cock

Epilepsy Group, Clinical Neuroscience, St Georges Hospital Medical School, London, UK

Status epilepticus (SE) is a medical emergency that can result in permanent neurological damage (particularly to the hippocampus) and mental disability. Mitochondrial dysfunction has been implicated in the neuronal damage seen following SE (Cock et al. 2002). Levetiracetam (LEV) is a novel antiepileptic drug that has shown potential as a therapeutic agent for the treatment of SE (Mazarati et al. 2004) and is known to be neuroprotective (Hanon & Klitgaard 2001). Here we examine mitochondrial dysfunction in the hippocampus following SE and the effects of LEV. Perforant path stimulation was used as a model of SE; rats were anaesthetised with halothane and stimulating and recording electrodes were implanted stereotactically into the right perforant pathway and dentate granule cell layer respectively. 6 days later, the unanaesthetised, animals underwent 2h of perforant path stimulation (2-4mA at 20Hz) before i.p. administration of LEV (200mg/kg) or saline (1.2ml/kg). Self-sustaining chronic limbic status ensued, and continued for 3h before termination by diazepam (20mg/kg, i.p.). 44h later the rats were sacrificed humanely and both hippocampi extracted and dissected into 3 regions (CA1, CA3 and dentate gyrus). Spectrophotometric assays were performed on the samples to measure levels of mitochondrial respiratory chain and matrix enzymes in sham rats (n=8) compared to SE rats which received saline (n=5) or LEV (n=5). Additionally, levels of reduced glutathione (an antioxidant) were measured using electrochemical HPLC.
When compared to shams, levels of mitochondrial enzymes and glutathione in the hippocampal regions were significantly reduced in the SE rats that received saline (see table). Citrate synthase and complex II/III were unaffected. This specific pattern of biochemical change confirms earlier findings with this model (Cock et al. 2002) and supports the notion that cell death following SE involves oxidative stress and excitotoxic mechanisms. Administration of LEV did not significantly protect against these biochemical changes (see table). Further experiments are underway to assess the influence of higher doses of LEV.

Hippocampal region	CA1		CA3		Dentate gyrus	
Treatment	SE + saline	SE + LEV	SE + saline	SE + LEV	SE + saline	SE + LEV
Complex I	-20% ***	-21% ***	-18% ***	-13% ***	-23% ***	-19% ***
Aconitase	-23% ***	-26% ***	-31% ***	-34% ***	-21% ***	-23% ***
α-ketaglutarate dehydrogenase	-16% ***	-16% ***	-27% ***	-29% ***	-17% ***	-18% ***
Glutathione	-16% ns	-13% ns	-25% ***	-19% ***	-28% ***	-28% **

Percentage change in mitochondrial enzymes and glutathione levels following perforant pathway stimulation and treatment with saline or LEV compared to sham animals, one way ANOVA and LSD ***p<0.005, **p<0.01.

Cock et al. (2002) Epilepsy Research 48 157-168.

Mazarati et al. (2004) Epilepsy Research 58 167-174

Hanon & Klitgaard (2001) Seizure 10 287-293

Study funded by UCB Pharma

Where applicable, the experiments described here conform with Physiological Society ethical requirements.

PC63

Scaffolding proteins in the olfactory epithelium

M. Saavedra[1], K. Castillo[1], U. Thomas[2], E. Gundelfinger[2], U. Wyneken[3] and J. Bacigalupo[1]

[1]U. of Chile/Millenium Inst. CBB, Santiago, Chile, [2]Leibniz Inst. for Neurobiology, Magdeburg, Germany and [3]U. Los Andes, Santiago, Chile

The olfactory system discriminates among thousands of odorants. Odor transduction occurs in the chemosensory cilia of olfactory receptor neurons (ORNs). Odorants induce excitatory or inhibitory responses, characterized by increases or decreases in firing rate, respectively. Both response types can be generated by a single ORN and are thought to involve G-protein coupled odor receptors that trigger a cAMP cascade, activating cyclic nucleotide gated-channels. A Ca^{2+} influx through such channels activates depolarizing Ca^{2+}-dependent Cl^- channels, in the first case, and hyperpolarizing Ca^{2+}-dependent K^+ channels, in the second situation. We investigated the presence of scaffolding proteins in the olfactory epithelium, because such proteins could be involved in the organization of the transduction apparatus. This would have important physiological implications. Scaffolding proteins like MAGuKs (membrane-associated guanylate kinase homologs) contain PDZ (PSD95/Dlg/ZO homolog), SH3 (Src homolog) and GuK (Guanilate kinase homolog) domains that mediate protein-protein interactions. The PSD95/SAP90 family of MAGuKs has 4 homolog members: PSD95/SAP90, SAP97/Dlg, SAP102/NE-dlg and Chapsyn110/SAP93.
We isolated a subcellular fraction of olfactory cilia, as indicated by specific markers. Epithelia were obtained from adult rats killed by an anaesthetic overdose (pentobarbitone 60 mg/Kg ip), according to the guidelines of the Ethics Committee of the University of Chile. Western blots showed several bands between 33 and 120 kDa, reactive to an antibody against PDZ domains of the PSD95/SAP90 family. These bands were present in the ciliary fraction, and some of them were absent in forebrain homogenates (positive controls), suggesting that they may correspond to new isoforms or to postranslationally modified proteins of the PSD95/SAP90 family (5 times). When we tested specific antibodies against each member of the PSD95/SAP90 family, PSD97 was detected (twice), whereas an anti-SAP102 antibody revealed a band with a smaller molecular weight than in the forebrain (4 times). In RT-PCR experiments with cDNA from the olfactory epithelium (twice), we used specific primers for several regions of neuronal SAP102. The results support the presence of a SAP102 sequence with deletions in the HOOK region connecting the PDZ3 and SH3 domains. The deletions are either in exon 2 or 14 and may account for the lower molecular weight species in the Western blots.
Our results suggest that scaffolding proteins are present in olfactory cilia, where they may have a key role in transduction.

Supported by Mideplan ICM P99-031-F, Fondecyt 1020964, Mecesup UCH0012.

Where applicable, the experiments described here conform with Physiological Society ethical requirements.

PC64

Effects of MDMA on the induction of synaptic plasticity in visual cortex and hippocampus

C. Rozas[1], M. Encina[1], M. Reyes-Parada[2], F. Pancetti[1], B. Cassels[3] and B. Morales[1]

[1]Neuroscience Lab, Department of Biology, University of Santiago, Santiago, Chile, [2]School of Medicine, University of Santiago, Santiago, Chile and [3]Department of Chemistry, School of Sciences, University of Chile, Santiago, Chile

The amphetamine analog 3,4-methylenedioxymethamphetamine (MDMA, ecstasy), has become increasingly popular as a "recreational" drug, particularly among young people. Cognitive impairment has been associated with frequent use of MDMA in humans and learning deficits have been observed after chronic MDMA treatment in different animal models. These deficits might be related to the neurotoxic effect of MDMA on 5HT nerve terminals. It has also been shown in animal behavioral models that acute administration of MDMA can affect learning and memory. Nevertheless, there is no information regarding the effects of MDMA upon synaptic plasticity models as Long Term Potentiation (LTP) and Long Term Depression (LTD), which are involved in learning and memory processes. We studied the effect of acute application of MDMA on the induction of LTP and LTD in visual cortical brain slices and hippocampus. Slices 400 μm thick were obtained from 3-5 week-old Sprague-Dawley rats, killed by decapitation under halothane anesthesia according with the guidelines of the Ethics Committee of the University of Santiago, and maintained in artificial cerebrospinal fluid for 1 hr before recording. Field EPSPs were evoked with electrical stimulation using bipolar electrodes. For visual cortex, LTP or LTD were recorded in layer 2/3 after either tetanic or low frequency stimulation protocols applied to layer 4, respectively. For hippocampal slices, LTP or LTD was recorded in CA1 by stimulation applied from Schaeffer collaterals, using similar protocols. MDMA was superfused during 20 min (10 min before and after the electrical stimulation). Statistical significance for mean differences between experimental and control groups were assessed using Mann-Whitney U test. In the visual cortex LTP and LTD were inhibited of dose-dependent manner by MDMA. LTP was inhibited from +50± 3% (S.E.M., n=8) in control experiments to +20±3% (S.E.M., n=7) in sliced superfused with 50 μM MDMA ($Z=2.37$, $P<0.05$). LTD inhibition was from -35±10 % (S.E.M., n=5) in controls to -15±5%(S.E.M., n=5) in treated ($Z=-2.0$, $P<0.05$). Inhibition induced by MDMA was reverted removing the drug from the bath and after to apply a second tetanus. Interestedly and contrarily to expected, in hippocampus MDMA induced a doses-dependent increase in the induction of LTP. LTP in presence of 50 μM MDMA was of +170±25%(S.E.M., n=8),

where slice in control situation was of +50±3%(S.E.M., n=8; Z=-2.58, P<0.001). Non-significant effect was observed in LTD (Z=-0.85, P=0.39). These results show for the first time a direct effect of MDMA on the induction of LTP and LTD, which might be associated with the learning and memory deficits observed in human and animal models.

Fondecyt 1030220, Dicyt-USACH Grants.

Where applicable, the experiments described here conform with Physiological Society ethical requirements.

PC65

Modulation of Neuronal Proliferation and Differentiation by Nitric Oxide During Neurogenesis in Rat Olfactory Epithelium

L. Sulz[1], A. Mackay-Sim[4], R. Iturriaga[1] and J. Bacigalupo[2]

[1]Ciencias Fisiologicas, P.Universidad Catolica de Chile, Fac. de Ciencias Biologicas, Santiago, Chile, [2]Biologia, Universidad de Chile, Fac. de Ciencias, Santiago, Chile, [3]Millennium Institute for Advanced Study in Cell Biology and Biotechnology, Universidad de Chile, Santiago, Chile and [4]School of Biomolecular and Biomedical Sciences, Griffith University, Brisbane, QLD, Australia

The sensory neurons of the olfactory epithelium are continually renewed during the entire lifespan in mammals. The stem cells responsible for cellular replacement are among the basal cells of this epithelium (Mackay-Sim & Kittel, 1991). The enzyme nitric oxide synthase (NOS), which generates the diffusible messenger nitric oxide (NO), is transiently expressed during neurogenesis in the olfactory bulb and in the regenerating olfactory epithelium of adult animals (Roskams et al. 1994). To determine the role played by NO during olfactory neurogenesis, we used a serum-free system for culturing non-neuronal cells. Olfactory epithelia were obtained from adult rats sacrificed with an anaesthesia overdose (pentobarbitone 100 mg/Kg. ip). This protocol was approved by the ethics committee of all universities involved. We studied the presence of neuronal (nNOS), endothelial (eNOS) and inducible (iNOS) NOS isoforms, and the effects of NOS inhibitors and NO donors under conditions that promote proliferation or differentiation of olfactory epithelial cells *in vitro*. Proliferation and differentiation of the neuronal precursors were induced with fibroblast growth factor (FGF-2) and transforming growth factor (TGF-β2), respectively. We detected by immunocitchemistry the expression of the three enzyme isoforms under both conditions. Furthermore, we found that nNOS was present in tubulin βIII and neurofilament positive cells (immature neuronal markers) and in some GBC-1 positive cells (globose basal cells marker), but not in cytokeratin-14 positive cells (horizontal basal cells marker). In cultures treated with EGF/FGF-2 and TGF-β2, the proportion of cell in proliferation and differentiation determined by BrdU incorporation and neurofilament expression was 42.6±2.6% and 43.5±2.5%, respectively. The NOS inhibitors 1-2-trifluoromethylphenyl imidazole (TRIM) and L-N^6-1-iminoethyl-lysine (N-NIL) reduced proliferation and increased differentiation in a dose-dependent manner. However, 10-100 μM N-NIL (K_i 10 times lower than TRIM for iNOS), showed a stronger anti-proliferative effect (13.6±3.1% and 4.0±1.4% of control, respectively; p<0.05) than TRIM at the same concentration (63.2±5.6% and 39.2±2.9%). 100 μM SNAP increased the proportion of cells in proliferation (57.1±3.3%, p<0.05). Besides, we found iNOS, but not nNOS nor eNOS expression in the regenerating olfactory epithelium. These results support the idea that NO produced by iNOS participates in neurogenesis, stimulating basal cell proliferation in the olfactory epithelium, independently of cGMP.

Mackay-Sim, A and Kittel, P. (1991). J. Neurosci. 11, 979±984.

Roskams, D. et al. (1994). Neuron 13, 289±299.

Supported by a CONICYT doctoral fellowship (LS) and Mideplan ICM P99-031-F (JB)

Where applicable, the experiments described here conform with Physiological Society ethical requirements.

PC66

Permissive role for fibroblast-like cells in the induction of terminal Schwann cell sprouting at mouse neuromuscular junctions

F.A. Court, T.H. Gillingwater, P.J. Brophy and R.R. Ribchester

Centre for Neuroscience Research, University of Edinburgh, Edinburgh, UK

Previously we reported visualisation of a sub-population of fibroblast-like cells localised to neuromuscular junctions (NMJ), using polyclonal 2166-antibody (Court et al., 2003). We have now extended these observations by showing first, that the 2166 antibody probably recognises an unusual conformational form of tubulin. Second, immunocytochemical stains with CD34 antibody together with volume-rendered electron micrographs of a serially-sectioned NMJ from triangularis sterni (TS) muscles isolated from twelve mice killed by cervical dislocation (Home Office Schedule 1), showed extensive capping of motor endplates by the membranes of the 2166-positive junctional cells. Next, TS muscles were partially denervated by intercostal nerve section with Home Office authority in eight mice anaesthetised with ketamine/xylazine (respectively 100/10 mg/kg, IP). The mice were killed by cervical dislocation 1-6 days later. Muscles were isolated and prepared for whole-mount immunostaining. Within 24 hrs of nerve injury, 2166-positive cells had extended many fine cellular processes and this coincided with strong expression of tenascin C, a molecule implicated in the induction of motor nerve sprouting (Cifuentes-Diaz et al., 1998). By 3 days, terminal Schwann cells became reactive (nestin positive) and extended sprouts along 2166-positive cellular processes, pervading the tenascin-C positive extracellular matrix.

To test whether the 2166-positive cells play an instructive role in activating Schwann cells, we compared their responses to denervation with the effects of muscle paralysis. Botulinum toxin (type A; 2 ng/kg, SQ) was injected into the interstitial spaces internal to intercostal muscles of six ketamine/xylazine-anaesthetised mice and the muscles examined after killing the mice 1-6 days later. After 1 day, junctional fibroblasts sprouted to a level comparable to that in denervated muscles. The spread of 2166-positive cells continued over the following 5 days. However, terminal Schwann cells neither became nestin positive nor did they sprout within 6 days of TS muscle paralysis.

Together, these data suggest that the 2166-positive NMJ cells play a permissive role in triggering Schwann cell and motor nerve terminal sprouting. Stimuli independent of those that activate the junctional fibroblasts are required to activate terminal Schwann cells and induce them to sprout.

Cifuentes-Diaz, C et al. (1998) Cell Mol Biol 44, 357-379

Court, FA et al. (2003) J Physiol 548P, O48

We thank the MRC and Wellcome Trust for support; and A Thomson and D Thomson for expert technical assistance. F.A. Court was supported by a Wellcome Prize Studentship.

Where applicable, the experiments described here conform with Physiological Society ethical requirements.

PC67

Dichlorvos favors long-term potentiation in rat hippocampal slices: Involvement of the enzyme acylpeptide hydrolase

F. Pancetti, C. Olmos, C. Rozas, M. Zeise and B. Morales

Neurosciences Lab, Department of Biology, University of Santiago, Chile, Santiago, Chile

The organophospate dichlorvos (DDVP) is being used as an insecticide as well as in the therapy of cognitive deficits associated with Alzheimer disease in the form of the pro-drug metrifonate (Morris et al. 1998). Both uses depend on its capability to inhibit acetylcholinesterase (AChE) activity. However, a few years ago it has been reported that the enzyme acylpeptide hydrolase (ACPH) displays between 6 to 10 times a higher sensitivity to DDVP compared to AChE (Richards et al. 2000). ACPH catalyzes the hydrolysis of short peptides bearing an acylation in their N-terminal amino acid residue. The biological significance of this enzymatic activity has been elusive. Furthermore, there is a lack of information regarding of DDVP effects upon long-term potentiation (LTP). LTP have been accepted as a model of synaptic plasticity by which learning and memory processes might occur. The aim of our investigation is to test out the hypothesis that DDVP is involved in the enhancement of synaptic plasticity processes through a mechanism that involves ACPH. For these purposes, we studied the effect of acute application of DDVP on the induction of LTP in rat hippocampal slices. Briefly, Sprague-Dawley rats (3-5 weeks old) were sacrificed under anesthesia with halothane, as stated the bioethics protocols of the University of Santiago. Brains were rapidly removed and 400 μm thick slices were obtained using a vibratome. They were kept in gassed (95% CO2, 5% O2) artificial cerebrospinal fluid (ACSF) for at least one hour before recording. Field EPSPs were evoked with electrical stimulation using bipolar electrodes and recorded in the stratum radiatum of the CA1 hippocampal area. LTP was elicited by tetanic stimulation (5 trains, each with 10 bursts at 5 Hz, each burst having 4 pulses at 100 Hz) applied to Schaeffer collaterals. DDVP was applied by injection to the perfusion fluid during 20 min (10 min before and after the stimulation protocol), yielding a final concentration of 50 μM in the recording chamber. Recordings were acquired for 1 h after stimulation. Our results show that the mean of the potentiation achieved in the control condition is 107.9% + 23.3 (S.E.M., n=7), whereas in the slices exposed to DDVP the potentiation reaches a value of 219.1% + 39.9 (S.E.M, n=8); $P<0.05$ (two-tail, unpaired t-test). Surprisingly, the enzymatic activity of AChE from these slices was not affected by DDVP under the conditions previously described ($P=0.673$, n=3). Instead ACPH activity was 50% inhibited by DDVP ($P<0.0001$, n=3). These results support the notion that ACPH is a target of pharmacological and toxicological action of DDVP and suggest a possible role of ACPH in synaptic plasticity processes.

Morris, J.C., Cyrus, P.A., Orazem, J., Mas, J., Bieber, F., Ruzicka, B.B., Gulanski, B. (1998). Neurology 50: 1222-1230.

Richards, P.G., Johnson, M.K., Ray, D.E. (2000). Mol. Pharmacol. 58: 577-583.

Supported by DICYT-USACH to F.P.

Where applicable, the experiments described here conform with Physiological Society ethical requirements.

PC68

NITRIC OXIDE MODULATES THE ENHANCED BEHAVIORAL RESPONSE TO L-DOPA FOLLOWING REPEATED ADMINISTRATION IN THE 6-HYDROXYDOPAMINE-LESIONED RAT

F.E. Padovan-Neto[1], V. Tumas[3], M.Z. Gomes[2], E. Dias-de-Oliveira[1] and E. Del Bel[1]

[1]Physiology, FORP-University of Sao Paulo, Ribeirao Preto, Sao Paulo, Brazil, [2]Physiology, University of Sao Paulo-Medical School, Ribeirao Preto, São Paulo, Brazil and [3]Neurology, University of Sao Paulo-Medical School, Ribeirao Preto, Brazil

The enhanced behavioural response to repeated dopamine (DA)-replacement therapy seen in the 6-hydroxidopamine (6-OHDA)-lesioned rats has pharmacological characteristics similar to 3,4 dihydroxyphenyl-L-alanine (L-DOPA) induced dyskinesia (Henry et al., 1998; Lundblat et al., 2002). The neural mechanisms underlying L-DOPA-induced dyskenesia remain unknown. Nitric oxide (NO) has been proposed as a new neurotransmitter in the nervous system. Inhibition of NO synthase (NOS) induces an impairment of exploratory and motor behaviour and give support to the hypothesis that NO plays a role in motor behaviour control (Del Bel & Guimaraes, 2001). In addition results have shown an interaction between NO system and induced neurodegenerative process in nigrostriatal pathway (Gomes & Del Bel, 2003). In these experiments we examined the effects of an inhibitor of NOS on L-DOPA-induced-rotational behaviour in the 6-OHDA-lesioned rats and compare it to that of L-DOPA-induced dyskinesia. The experiments were carried out according to the Brazilian Society of Neuroscience and Behaviour guidelines for care and use of Laboratory animals. Male albino-Wistar rats (180-200 g) were housed in groups, in a temperature-controlled room with a 12-hour light/dark cycle, with free access to food and water. Rats with unilateral 6-OHDA lesions received single daily injections of L-DOPA (oral, 100mg/kg plus 15 mg/kg benserazide) for three weeks. The rats gradually developed abnormal involuntary movements, lasting 2-3 h following each L-DOPA dose. L-DOPA-induced rotation/2 h (1060.57±197.46) was potentiated

by the acute administration of the NOS inhibitor NG-nitro-L-arginine (L-NOARG, 50 mg/kg i.p.; 1746.28±261.58)) in 6-OHDA-lesioned rats. In contrast following priming by L-DOPA replacement therapy, administration of L-NOARG reduced L-DOPA-induced rotation/2 h (control=1156.8±350.52; L-NOARG=550±279.39). Within the L-DOPA-treated group, levels of NOS neurons in DA-denervated dorsal ipsilateral-striatum were higher in dyskinetic than in non-dyskinetic animals (NOS-neurons/100 μm^2, control=5.33±0.88; test=8.79±0.79). The results suggest that NOS-inhibitors may have anti-dyskinesogenic potential in Parkinson disease. It shown that L-DOPA-induced dyskinesia is associated with over-expression of NOS in the striatal projection neurons. Due to its treatment-dependent expression, striatal NOS may play a role in the mechanisms of behavioural sensitization brought about by the drug.

Henry, B et al., (1998) Exp Neurol 151: 334

Del Bel EA & Guimaraes FS (2000) Psycopharmacol 147:356

Lundblat M et al., (2002) Europ J Neurosc 15: 120;

Gomes MZ & Del Bel EA (2003) Brain Res Bull 62:107

Financial support FAPESP, CNPQ.

Where applicable, the experiments described here conform with Physiological Society ethical requirements.

PC69

Pseudorabies Virus-Assisted Identification of Neuronal Circuits Involved in Food Intake

C.A. Perez[1] and J.M. Friedman[2]

[1]The Rockefeller University, New York, NY, USA and [2]Howard Hughes Medical Institute, New York, NY, USA

Despite recent advances in the understanding of molecular events associated with energy homeostasis, higher-order brain centres responsible for eliciting and/or modulating food intake are not yet fully identified. This project has sought to discover brain areas that project toward peripheral organs involved in the food intake process (e.g. salivary glands, taste papillae, orofacial/lingual muscles, etc.) and to characterize the neurochemical properties of neurons in those brain regions. To achieve our objective we have identified neurons belonging to multiple neuronal circuits mapped by means of recombinant pseudorabies viruses (PRVs), a retrograde tracing agent, encoding various reporter proteins such as beta-galactosidase, green fluorescent protein (GFP) or red fluorescent protein (RFP).

PRV strains were injected in the following peripheral organs of male CB57BL/6J mice that had previously received an IP dose of ketamine/xylazine (60 mg/kg and 7 mg/kg, respectively): submandibular salivary gland, masseter muscle, and circumvallate taste papilla; in some cases we injected two different PRV strains in two different organs (n=3 or 4 for each group). Brains from infected mice were analysed by immunofluorescence microscopy. Brain areas identified by this approach, and belonging to multiple neuronal circuits, were defined as putative food intake control centers (FICCs). Our results indicate that discrete amygdaloid nuclei as well as some cortical structures (insular and rhinal cortices) are candidates to be FICCs. A further characterization of neuronal subtypes in FICCs is being performed by identification of PRV-infected neurons in transgenic mice lines expressing GFP in different subtypes of neurons, including those expressing the neuropeptide Y (NPY) and proopio-melanocortin (POMC).

Identification of good markers of FICC neurons and/or candidate genes to be involved in food intake regulation, will provide the basis to design ad hoc loss and gain of function studies aimed to probe the role of those candidate neurons and/or genes in determining the molecular and physiological mechanisms involved in the food intake process and the behavioral imbalances associated with eating disorders and ailments with high impact in our society, such as anorexia and obesity.

This work was supported by NIH grant RO1 DK041096. JF is a Howard Hughes Medical Institute Investigator.

Where applicable, the experiments described here conform with Physiological Society ethical requirements.